Research on the mechanism of elemental mercury removal over Mn-based SCR catalysts by a developed Hg-TPD method

Shibo Zhang[a,b], Mercedes Díaz-Somoano[b,*], Yongchun Zhao[a,*], Jianping Yang[c], Junying Zhang[a]

[a] State Key Laboratory of Coal Combustion, School of Energy and Power Engineering, Huazhong University of Science and Technology, Wuhan 430074, China.

[b] Instituto Nacional del Carbón (CSIC), Francisco Pintado Fe, 26, 33011 Oviedo, Spain.

[c] School of Energy Science and Engineering, Central South University, Changsha 410083, China.

*Corresponding author, Email: yczhao@hust.edu.cn, mercedes@incar.csic.es, Tel.: +86 27 87542417 , +34 985119090.

Abstract

Using SCR catalyst to oxidize and remove elemental mercury (Hg^0) synergistically is a promising method for mercury emission control in coal combustion power plants and is currently attracting widespread interest. In this study, a developed mercury thermal desorption (Hg-TPD) approach, combined with other associated methods, was employed for identification of the mercury species in the Mn-based SCR catalysts that have been used for synergistic Hg^0 removal. The analysis results demonstrated the Hg^0 adsorption on the catalysts was a necessary process for the Hg^0 removal, though the SCR catalysts removed Hg^0 mainly through catalytic oxidation and the amount of the adsorbed mercury contributed only a little to the Hg^0 removal efficiency. And the essential adsorption process was mainly in the way of chemisorption. HgO was the prime species that was identified to form in the catalysts, and a little amount of adsorbed $HgCl_2$, $Hg(NO_3)_2$ and Hg-OM was detected as well in the samples spent in the simulated coal-fired flue gases. O_2, HCl, NO and high concentration of CO_2 in the flue

gas all promoted the adsorption capacity and the generation of related Hg compounds so that they were conductive to Hg^0 removal efficiency, while similar phenomenon was not emerged in the presence of SO_2, NH_3 and H_2O and meanwhile the amount of adsorbed HgO was decreased so that the efficiency was inhibited. The mobility testing by sequential extraction procedure indicated most of the retained Hg belonged to the mobile fraction, which was in accordance with the identification results of the Hg-TPD analysis. The consequences of this research would create a better understanding of the Hg^0 removal mechanism over the Mn-based SCR catalysts and provide additional information on the disposal of the retired catalysts in the environment.

Keywords: SCR catalyst; Hg-TPD; mercury species; mobility; mechanism

1. Introduction

Mercury emissions continue to be one of the most important worldwide concerns due to the bioaccumulation and persistence of mercury in the environment. The Minamata Convention that entered into force on 16 August 2017 becomes into the first international legally binding treaty to prevent mercury emissions. The primary objective of the convention is to "protect human health and the environment from anthropogenic emissions and releases of Hg and Hg compounds". This agreement infers specific guidelines in industrial emissions and underlines the need for innovative approaches and the transfer of technology to avoid this problem.

As one of the largest anthropogenic mercury emission sources, coal-fired power plant is focused on in recent years for its mercury control. Mercury emitted from coal combustion process exists mainly in three forms: i) elemental mercury (Hg^0), ii) oxidized mercury (Hg^{2+}) and iii) particle-bond mercury (Hg^p).[1-3] Hg^p can be easily removed by particle control devices such as electrostatic precipitators or fabric filters while Hg^{2+} is soluble in water and can be easily captured by wet flue gas desulfurization

(WFGD) scrubbers.[3-5] However, Hg^0 is very volatile and insoluble in water so that it is difficult to be controlled by the existing air pollution control devices (APCDs) of the power plants.[6,7] The effect of mercury control that can be achieved with each of these approaches is extremely variable, which ranges from 43.8% to 94.9%, and it is affected by such factors as coal chemistry or operational conditions.[1,8] As emission limits have been tightening and new pollutants (mercury, trace metals, halogens, fine particulates) become targeted, it is mandatory to work with the existing systems to enhance the synergistic multi-pollutant controls besides the development of specific mercury control technologies.

Currently, a commercially available technology for controlling the mercury emission from coal-fired flue gas is the injection of activated carbon. Usually this method has certain effect on Hg^0 removal, especially when the activated carbons are pretreated with mineral acid (H_2SO_4, HNO_3 or $HClO_4$) or sulfur.[9,10] However, the injection of activated carbon has some problems such as the relative high cost of this technology due to the large amount of activated carbon requires and the risk of compromising fly ash quality.[11] To avoid these drawbacks, an alternative approach is to develop the co-benefit of installed devices for the elimination of other pollutants and specifically the oxidation of Hg^0 to Hg^{2+} which can then be captured by downstream WFGD. Among the existing equipments, selective catalytic reduction (SCR) systems which are installed for the NO_x emission control in coal-fired power plants were reported to have the capacity to oxidize Hg^0 to Hg^{2+} because of the existence of active oxygen on the SCR catalyst surface.[12] Related literatures have investigated and confirmed the Hg^0 oxidation ability of the commercial vanadium-based SCR catalyst, especially in the flue gas containing high concentration of HCl.[13,14] Other novel SCR catalysts which were developed in recent years, such as Ce-based and Cu-based

catalysts, exhibited relatively high Hg^0 removal activity as well in proper modifying and flue gas conditions.[15-18] In our previous studies, Mn-based catalysts were investigated as a kind of novel SCR catalyst. The results demonstrated the catalysts owned excellent performance for NO removal and synergistic Hg^0 removal and were applied in various simulated coal combustion flue gas.[19-22] Besides, an obvious advantage of Mn-based catalysts compared to most of the others was the lower working temperature. This feature made it feasible to put the catalyst more downstream in the flue gas, which was favorable for the life span of the catalyst and the heat recovery efficiency of the whole power plant. In addition, Scala et al.[23,24] also demonstrated in the aspect of reaction kinetics that the Mn-based sorbent had remarkable mercury capture and oxidation ability in the temperature range of less than 300℃, especially in the presence of HCl. However, in spite of these advantages, the Hg^0 removal efficiency showed a wide variability with the changes of the experimental parameters such as the specific components of the catalysts, operational temperature and flue gas components. There was no general agreement on the influences of these parameters on the efficiency, and the mechanism for the Hg^0 removal over the Mn-based catalysts was still not completely understood.

In the past few years, a developed mercury thermal programmed desorption (Hg-TPD) method was demonstrated to be qualified for mercury species identification and mechanism analysis on the Hg^0 removal with solid samples.[25,26] So far, several kinds of solid samples referring to mercury migration and transformation, such as coal,[27,28] fly ash,[29,30] gypsum,[31] Hg sorbents[27,32-35] and Hg-contaminated soil and sediments[29,36], have been analyzed by the Hg-TPD approach for identifying the Hg species on them, and some important conclusions about the Hg^0 removal mechanism and the influences of Hg transfer on the environment were acquired. For instance, through Hg-TPD, N.

Fernández-Miranda et al.[30] investigated the mercury retention in fly ashes obtained from coal combustion and acquired that mercury was captured through forming mercury bound to organic matter and HgS in the fly ashes. M. Rallo et al.[33] found that Cl and S were the dominant factors for the Hg retention by biomass chars which served as a kind of mercury sorbent because mercury chlorine and mercury sulfate were the main produced species in the capture process. M. Rumayor et al.[31] concluded that the primary mercury species present in WFGD gypsum was HgS which was chemically stable and not easily released to the environment. And Hg species retained in soil and sediments sampled around old mining-metallurgy sites was also mostly in stabilized states so that the effect of the Hg-contaminated soil and sediments on the environment was limited as well.[36] However, although there have already been numerous researches in this field, little literatures have focused on the Hg-TPD analysis on SCR catalyst which acted as an important role in mercury emission reduction. And similarly with the existing studies, the analysis results are potentially valuable for revealing related mechanisms of the Hg^0 removal over SCR catalysts. Hence, in order to fill in the gaps, the present study was carried out to use the Hg-TPD approach, combined with other associated methods, to analyze the spent SCR catalysts.

Specifically, in this work, the Mn-based SCR catalysts that have been used for evaluating their Hg^0 removal performance in our previous study were selected as the analyzed samples for the purpose of carrying on the previous research. The methods of Hg-TPD, mercury content measurement and sequential solution extraction were all employed for analyzing the Hg-loaded catalysts, and the speciation, amount and mobility of the formed mercury species in the catalysts were identified. The testing results will present a better understanding of the Hg^0 removal mechanisms over the SCR catalysts and also the effects of the spent catalysts on the environment, which is helpful

for developing SCR catalyst with high catalytic efficiency and the eco-friendly disposal of the retired catalysts.

2. Materials and methods

2.1. Samples

Three kinds of previously evaluated Mn-based SCR catalysts, MnO_x/TiO_2, Fe-MnO_x/TiO_2 and $CeMnO_3$, were employed for the present analysis research. The catalysts were all prepared by the sol-gel method of which the procedures have been introduced in our previous studies.[19-22] Then they were evaluated for Hg^0 removal in different flue gases. Specifically, the MnO_x/TiO_2, Fe-MnO_x/TiO_2 and $CeMnO_3$ catalysts were reacted in the air combustion simulated flue gas, and the spent catalysts were labeled as MnTi-air, FeMnTi-air and CMO-air, respectively. MnO_x/TiO_2 was additionally reacted in the oxy-fuel combustion simulated flue gas, with MnTi-oxy as the label of this spent catalyst. Besides, another nine spent samples derived from the $CeMnO_3$ catalyst reacted in the individual flue gas components were also collected for the analysis. All of these selected samples were operated to perform the Hg^0 removal experiments at 200℃ which was the lower limit of the optimal temperature range for the SCR deNO_x reaction.[19-22] In summary, the thirteen Hg^0-loaded samples in total were the analysis objects of this work.

2.2. Identification of Hg species by thermal desorption

An optimized thermal desorption approach was mainly utilized in this work for identifying the mercury species in the samples. The equipment employed for this procedure was a modified version of a commercial device, which has been described in the previous works,[25,27,29] and the whole analytic system was shown in Figure 1. In the course of the Hg-TPD analysis, 20mg of the sample was placed in the decomposition furnace where desorption of the mercury species was carried out in nitrogen atmosphere

to avoid any interferences and undesired reactions. Hg species were released from the solid matrix in the N_2 flow with a rate of 500mL/min. The heating mode was controlled at approximately 50℃/min^{-1} by a temperature controller. The desorbed mercury species were then transported to a commercial PYRO furnace kept at 800℃ where 500mL/min O_2 was introduced. In this unit, the mercury compounds were reduced to elemental mercury and the added O_2 was used to oxidize volatile matter of which the existence would impact the monitor of mercury. In order to prevent the interference of the oxidation of volatile matter on the desorption of mercury species, O_2 was introduced to the PYRO furnace, rather than to the decomposition furnace together with the introduction of N_2. The PYRO was connected to the decomposition furnace by an additional chamber which was designed to ensure that the temperature was maintained so as to avoid cool zones and the condensation of the mercury before it entered the PYRO furnace. The elemental mercury in gas phase was finally determined using a RA-915+ analyzer from Lumex based on differential Zeeman atomic absorption spectrometry. This equipment recorded the mercury signal versus the temperature of the decomposition furnace. The obtained desorption profiles were compared with those of the reference mercury compounds of which the temperature parameters of thermal release were obtained previously and presented in Table 1.[34] Through the comparisons, the mercury species were identified from the temperature range in which the thermal release occurred, especially the high peak temperature.

2.3. Determination of total mercury content

An automatic mercury analyzer from LECO (AMA 254) which is based on atomic absorption spectrometry was employed to determine the total mercury content in the spent catalysts. For each testing, the sample with a weight of 20mg was put into a nickel boat, followed by the ordinal processes of dried at 120℃ for 70 seconds and

combusted in an oxygen atmosphere at 750℃ for 150 seconds. Then the released mercury was detected and the total mercury content was finally obtained.

2.4. Sequential extraction procedure

A sequential extraction procedure based on a simplification of the US Environmental Protection Agency Method 3200 was also employed for identifying the speciation and mobility of the mercury loaded on the spent samples. This method was to utilize the distinct solubility of mercury species in different solutions. Specifically, three extraction solutions with each volume of 1.5mL were sequentially passed through the solid sample with a dosage of 50mg. The sample residue was rinsed by 0.5mL deionized water between each sequential step. The resulting solutions were analyzed by AMA 254 to detect the mercury contents, and the proportion of each of the three mercury fractions which were introduced in Table 2 among the total loaded mercury in the sample was acquired. All of the extraction solutions used in this procedure were prepared with mercury-free reagents.

3. Results and discussion

3.1. Hg-TPD analysis on the spent Mn-based SCR catalysts

In our previous studies, the results of evaluations on Hg^0 removal performance indicated that the Hg^0 removal efficiencies over the Mn-based SCR catalysts (MnO_x/TiO_2, Fe-MnO_x/TiO_2 and $CeMnO_3$) showed a decreasing trend overall with the increase of the reaction temperature.[20-22] As high temperature was apparently adverse to the Hg^0 adsorption, a reasonable explanation was that Hg^0 adsorption on the catalysts was a necessary process for the Hg^0 oxidation and removal.[16,37] And all the mercury retained in the catalysts could be considered to derive from the adsorbed Hg^0 (Hg^0_{ad}). Therefore, identifications of the adsorbed mercury species over the catalyst samples that have been spent for the evaluations on their Hg^0 removal efficiency were very likely to

be helpful for acquiring related mechanisms of the Hg^0 removal over the catalysts, which was what this research was mainly devoted to using Hg-TPD approach.

3.1.1. Analysis on the catalysts spent in simulated coal combustion flue gas

The Hg-TPD analysis was first carried out on the catalysts spent in the simulated coal-fired flue gases (air combustion: N_2+4%O_2+12%CO_2+10ppmHCl+400ppmSO_2+ 400ppmNO+400ppmNH_3+10%H_2O+70μg/m^3Hg^0, oxy-fuel combustion: N_2+4%O_2+ 70%CO_2+10ppmHCl+400ppmSO_2+400ppmNO+400ppmNH_3+20%H_2O+70μg/m^3Hg^0), and the desorption profiles of MnTi-air, MnTi-oxy, FeMnTi-air and CMO-air were shown in Figure 2(a), (b), (c) and (d), respectively. The integral area of the profiles and the previously measured Hg^0 removal efficiencies of the catalysts in the simulated flue gases were summarized in Table 3. The Hg^0 removal efficiency was defined as the ratio of the decreased Hg^0 concentration among the initial Hg^0 concentration, and it was obtained when Hg^0 concentration in the downstream gas of the catalyst reached stability. Because of the stability, the spent catalysts was in the state of Hg saturation and the testing results could not only reveal the Hg species but also reflect the Hg adsorption capacity of the catalysts. Comparing the desorption profiles of the four samples, the peak intensity followed the order: MnTi-air < MnTi-oxy < FeMnTi-air < CMO-air, indicating the CO_2 enrichment, Fe modification and perovskite-type structure were all favorable for the Hg^0 adsorption. This intensity sequence could be more intuitively reflected by the integral area of the profiles, and the result coincided with the Hg^0 removal efficiencies, which further proved the significance of the adsorption process. Among the catalysts, $CeMnO_3$ exhibited the strongest Hg^0 adsorption ability. However, according to the characterization results as summarized in Table 4, the surface area, pore volume and pore size of $CeMnO_3$ were much smaller than those of MnTi and FeMnTi because of the higher calcination temperature during the preparation.[21,22]

Instead, the proportion of chemisorbed oxygen (O_{ad}) among total O species in $CeMnO_3$ was obviously higher than those in the other two catalysts on the premise that the atomic concentrations of element O in the three catalysts were close to each other. So the largest advantage of $CeMnO_3$ was the abundant chemisorbed oxygen on the surface, which was derived from oxygen transfer between the Ce^{3+}/Ce^{4+} ion pair in the catalyst.[22] Thus, it could be concluded from the results that the necessary Hg^0 adsorption process was realized mainly through chemisorption rather than physisorption. And the chemisorption of Hg on Mn-based catalyst was confirmed by the kinetic analysis method of Scala et al. as well.[23,24]

Then, according to the results in Figure 2(a)-(d), there were desorption peaks emerging at about 150℃, 275℃ and 472℃ in all the four profiles, which were identified as $HgCl_2$, $Hg(NO_3)_2$ and HgO, respectively, through referring to the high peak temperature of the pure Hg compounds shown in Table 1. It demonstrated that the elemental mercury was removed over the catalysts through being oxidized to the three Hg compounds in both the simulated flue gases. Among the generated Hg compounds, HgO was the main formed mercury species that adsorbed on the catalyst because of its obviously stronger desorption peak intensity than the others'. This could be owed to the higher desorption temperature of HgO which made its adsorption bonds more forceful. By contrast, the intensity of the peaks corresponding to $HgCl_2$ and $Hg(NO_3)_2$ were much weaker. On one hand, the concentrations of HCl and NO in the flue gas were as low as the magnitude of ppm so that the generation amount of $HgCl_2$ and $Hg(NO_3)_2$ were small; On the other hand, both $HgCl_2$ and $Hg(NO_3)_2$ were volatile,[15] and meanwhile their desorption temperatures were close to or even lower than the reaction temperature used for evaluating the Hg^0 removal performance of the catalysts (200℃). Due to these reasons, the adsorption of $HgCl_2$ and $Hg(NO_3)_2$ on the catalysts was

relatively difficult. In addition, on the profile of MnTi-oxy, an additional peak could be found to exist at about 210-220℃, which corresponded to the desorption of Hg-OM (Hg bound to organic matter). Related literatures have indicated that the high concentration of CO_2 in oxy-fuel flue gas promoted the forming of -COOH, C-O and C=O which belonged to the organic functional groups that mercury could adsorb on, therefore favoring the formation of Hg-OM.[20,38,39] And some mineral acid generated under the high-content H_2O condition could assist this adsorption process.[40,41] In spite of the various formed mercury species, it should be noted that there were no Hg compounds containing sulfur, such as HgS and $HgSO_4$, adsorbed on the samples in the presence of SO_2. This phenomenon was mutually verified with the previous finding that SO_2 had inhibitive effects on the kinetic constant of Hg^0 removal reaction over the Mn-based catalysts and led to the decreased Hg^0 removal efficiencies, which was mainly due to the deactivation of the catalysts resulted from the active Mn species reacted by SO_2 to form $MnSO_4$.[16,19-22,24,42]

Furthermore, the total contents of adsorbed mercury in the spent samples were also measured by AMA analyzer, and the results were shown in Table 3 as well. From the table, it was found that the adsorbed Hg contents were in proportion to the area of the desorption peaks and the Hg^0 removal efficiencies of the catalysts, which demonstrated the reliability of the test results. According to the results, the mercury contents in the spent samples were in the range of 0.915-1.482ppm. However, the total amounts of the removed mercury over the catalysts corresponding to the catalyst dosages in the previous Hg^0 removal experiments was calculated to be at least 10ppm.[20-22] Hence, it could be concluded that the adsorbed mercury contributed only a little to the Hg^0 removal efficiency though the adsorption procedure was essential. And the Hg^0 removal over the SCR catalysts was mainly in the approach of Hg^0 oxidation followed

by the oxidized mercury species released to the flue gas. In this way, the maintenance of the Hg^0 removal efficiency was guaranteed.

3.1.2. Analysis on the $CeMnO_3$ catalyst spent in individual flue gas components

The catalyst samples spent for the Hg^0 removal in individual flue gas components were analyzed by the Hg-TPD method as well. In this section, the $CeMnO_3$ catalyst was selected as the representative sample for the analysis because of its prominent Hg^0 adsorption capacity and catalytic efficiency, which could make the comparison between the analysis results of the samples spent in different atmospheres relatively clear. The desorption profiles and the calculated integral area of them were shown in Figure 3 and Table 5, respectively. The previously evaluated Hg^0 removal efficiency of the $CeMnO_3$ catalyst in each atmosphere was summarized in Table 5 as well. According to the results in Figure 3, it was apparent that the desorption peak corresponding to HgO with relative large intensity emerged in all of the profiles. So HgO was the dominant Hg species retained in the samples, which was in consistence with the desorption profiles of the samples spent in the simulated flue gases. With the addition of $4\%O_2$ into pure N_2 for Hg^0 removal in the previous experiment, the intensity of the HgO peak of the spent sample became stronger as reflected by comparing the profiles in Figure 3(a) and Figure 3(b). The existence of O_2 in the reaction gas improved mercury adsorption ability of the catalyst, therefore promoting the Hg^0 removal efficiency as reflected in Table 5. As 10ppmHCl was further introduced, the peak representing the desorption of $HgCl_2$ emerged as shown in Figure 3(c), indicating that Hg^0 was oxidized by HCl to form $HgCl_2$. HCl could generate active Cl on the catalyst surface which had stronger oxidability than the surface oxygen.[13,43] As a result, some mercury that was originally adsorbed in the form of HgO converted to $HgCl_2$, making the HgO peak become weaker compared to that of the sample reacted in only N_2+$4\%O_2$.

The weakness of the $HgCl_2$ peak was due to the volatility of $HgCl_2$ and the low desorption temperature which make most $HgCl_2$ released as gaseous Hg^{2+}. Associated with the relative weak HgO and $HgCl_2$ peak, the integral area and retained Hg content inversely showed a little smaller values than those of the sample spent in N_2+4%O_2, but it did not affect the facilitation of HCl on Hg^0 removal efficiency. The promotion of HCl on Hg^0 removal to form $HgCl_2$ was also demonstrated by the results of kinetic analysis of Scala et al.[24] Similarly with HCl, the introduction of NO likewise led to the emergement of a weak desorption peak at approximately 280℃ as shown in Figure 3(e). Although the desorption temperature was close to those of both $Hg(NO_3)_2$ and HgO yellow, the peak could be guaranteed to correspond to $Hg(NO_3)_2$ rather than HgO yellow because it was not emerged on the profiles of the samples spent in the atmospheres without NO. And by this way, the peaks at similar temperature in Figure 2(a)-(d) were judged to be $Hg(NO_3)_2$ as well. In the presence of O_2, NO could be oxidized to NO_2 which was also a kind of efficient oxidant, followed by Hg^0 being oxidized by NO_2 to form $Hg(NO_3)_2$.[15,22] This was the reason for the presence of the $Hg(NO_3)_2$ peak and the promotion of NO on the Hg^0 removal efficiency. However, differently from the outcomes after the additions of O_2, HCl and NO, none of the introductions of SO_2, NH_3 and H_2O brought about the emergement of new desorption peaks. Meanwhile, the intensity of the original peaks declined obviously compared to those before these components were introduced, as shown in Figure 3(d), Figure 3(f) and Figure 3(g). Thus, the addition of each of SO_2, NH_3 and H_2O into the reaction gas would cause the decrease of the Hg^0 adsorption capacity of the catalyst, which was adverse to the Hg^0 removal activity. This statement could be confirmed by the data of Hg^0 removal efficiency presented in Table 5. In addition, the effect of CO_2 was also analyzed. As 12%CO_2 was introduced, the desorption profile (shown in Figure 3(h))

showed little variation compared to that of the sample spent in N_2+4%O_2. When the CO_2 concentration increased to 70% in the flue gas, the intensity of the HgO peak slightly enhanced (shown in Figure 3(i)). These descriptions could be reflected more clearly by the integral area of the profiles. Meanwhile, a small peak corresponding to Hg-OM was formed at 228℃ in the profile of the sample spent in the presence of 70%CO_2, which was in accordance with the results in Figure 2(b) and further demonstrated the promotion of the CO_2 enrichment on the generation of Hg-OM and the Hg^0 adsorption capacity. And this was just the reason for the higher Hg^0 removal efficiency in oxy-fuel combustion simulated flue gas than in air combustion simulated flue gas.

The total mercury contents in the $CeMnO_3$ samples after spent for Hg^0 removal in individual flue gas components were likewise tested, and the results were presented in Table 5. It showed that the mercury contents in the spent samples were mostly lower than 1ppm. The low level of the adsorbed mercury amount was in consistence with the results in Table 3. Nevertheless, what should be paid attention to was that the adsorbed mercury content was in the same variation trend overall with the Hg^0 removal efficiency with the introduction of each component into the reaction gas, which demonstrated the importance of the Hg^0 adsorption process for the Hg^0 removal over the catalyst once again.

3.2. Sequential extraction procedure over the spent Mn-based SCR catalysts

The method of the sequential extraction procedure was also employed for identifying the mercury species in the SCR catalysts, and the samples spent in the simulated flue gases were tested. Through this method, the mobility of the mercury species retained in the catalysts was obtained, and it was helpful for predicting the impact of the disposal of the retired SCR catalysts on the environment. The test results

were shown in Figure 4. Most of the mercury in the spent samples was extracted from the mobile fraction, while little was detected in the non-mobile fraction. This consequence was in accordance with that of the Hg-TPD analysis by which the mercury species in the catalysts was identified to occur mainly in the forms of HgO, $HgCl_2$ and $Hg(NO_3)_2$. All of the species of HgO, $HgCl_2$ and $Hg(NO_3)_2$ belongs to the mobile fraction extracted in the procedure referring to the information presented in Table 2. Besides, the result of MnTi-oxy showed a larger proportion of semi-mobile Hg than those of the other samples. This phenomenon further demonstrated the generation of Hg-OM which belongs to the semi-mobile fraction in the sample reacted in the oxy-fuel combustion simulated flue gas.

Because of the superior mobility of the adsorbed mercury in the catalysts, the retained Hg was easy to migrate from the catalysts, and then it might transform to bioavailable Hg compounds such as methyl-Hg.[36] Hence, it was severely harmful to the ecotope if the retired catalysts were disposed in the environment directly. As the mobile fraction occupying the majority of the total retained Hg, an effective approach for lowering the environmental impact might be to pretreat the retired catalysts with the solution of 2%HCl+10%ethanol to remove the mobile Hg before disposing them in the environment. Then the rest of the mercury was only in a small amount and it was theoretically semi-mobile or non-mobile so that the migration was not easy to occur. In order to evidence this inference, the Hg-TPD analysis was additionally carried out over the samples after the first step of the extraction. The desorption profiles shown in Figure 5(a) displayed that the intensity of the desorption peaks reduced dramatically to very low level after the spent samples have undergone the extraction of F1 except the persistence of a Hg-OM peak on the profile of MnTi-oxy at about 220℃, indicating that most of the retained Hg was taken away. This result verified the effectiveness of the

pretreatment method mentioned above, and it also demonstrated the reliability of the extraction procedure. Then, the total mercury contents in the samples were also measured for quantitative analysis, and the results were presented in Table 6. It reflected that the mercury contents in the four samples were no more than 0.171ppm, which dropped significantly compared to those before the extraction process. The decline of the Hg content in MnTi-air, FeMnTi-air and CMO-air all exceeded 90%, while it was a little lower in MnTi-oxy because of the existence of Hg-OM as the semi-mobile Hg. Nevertheless, the decreasing range of that in MnTi-oxy was still as high as 85.5%. Thus, in conclusion, the one-step extraction process in advance was an effective method to reduce the content and mobility of the mercury in the spent SCR catalysts, therefore alleviating the harmful influence of their disposal on the environment. Furthermore, the samples that have suffered the complete three steps of the extraction procedure were also tested by the Hg-TPD analysis, with the results shown in Figure 5(b). It showed that the epibiotic peaks on the desorption profiles of the samples after the extraction of F3 further became weaker compared to those after the extraction of F1 and they were almost disappeared, including the peak corresponding to Hg-OM. So the results further proved the validity of the sequential extraction procedure.

3.3. Mechanism of Hg^0 removal over the Mn-based SCR catalysts

Summarizing the analysis results obtained above, related mechanisms of the Hg^0 removal over the Mn-based SCR catalysts could be concluded. First, gaseous Hg^0 ($Hg^0(g)$) was adsorbed on the catalysts to form adsorbed Hg^0 (React. 1), which was the necessary process for the Hg^0 removal. Then the Hg^0_{ad} was reacted, and HgO was the essential product of the catalysis because its desorption peak showed the strongest intensity and was found in each flue gas. Besides HgO, $HgCl_2$ and $Hg(NO_3)_2$ were also found to be generated in the presence of HCl and NO, respectively. The discovery of the

forming of adsorbed HgO, $HgCl_2$ and $Hg(NO_3)_2$ in individual flue gas components verified the analysis results of the mercury species in the catalysts spent in simulated coal-fired flue gases. Thus, Hg^0 removal over the catalysts in coal combustion flue gas was mainly through the adsorbed Hg^0 being oxidized to HgO, $HgCl_2$ and $Hg(NO_3)_2$, and the mechanism equations could be described as React. 2-4.[22,44-46] In these processes, the active oxygen (O*) in the catalysts played an important role, which could be replenished by gaseous O_2 (React. 5).[47] Furthermore, Hg-OM was additionally formed in the condition of CO_2 enrichment, such as oxy-fuel combustion flue gas. Some organic functional groups, such as C-O and C=O, were the important intermediates in this reaction.[34] And the high concentration of CO_2 was also favorable to the generation of HgO.[38,39] So the additional involvement of CO_2 on the Hg^0 removal in oxy-fuel combustion flue gas was described as React. 6 and 7. It should be pointed out that the formed HgO, $HgCl_2$ and $Hg(NO_3)_2$ were in the adsorption state in the beginning (with the subscript of "ad"), and then they were released into the flue gas as gaseous oxidized mercury, as described by React. 8-10,[48,49] which was demonstrated by combining the results of Hg-TPD analysis, retained Hg content measurement and total removed Hg^0 amount calculation.

$$Hg^0(g) \rightarrow Hg^0_{ad} \quad (1)$$

$$Hg^0_{ad} + O^* \rightarrow HgO_{ad} \quad (2)$$

$$Hg^0_{ad} + 2HCl + O^* \rightarrow HgCl_{2\,ad} + H_2O \quad (3)$$

$$Hg^0_{ad} + 2NO + 2O_2 \rightarrow Hg(NO_3)_{2\,ad} \quad (4)$$

$$O_2 \rightarrow 2O^* \quad (5)$$

$$CO_2 + C=C \rightarrow C-O, C=O \quad (6)$$

$$Hg^0_{ad} + C-O, C=O \rightarrow Hg\text{-}OM + HgO + C=C \quad (7)$$

$$HgO_{ad} \rightarrow HgO(g) \quad (8)$$

$$HgCl_{2\,ad} \rightarrow HgCl_2(g) \quad (9)$$

$$Hg(NO_3)_{2\,ad} \rightarrow Hg(NO_3)_2(g) \quad (10)$$

Besides the reaction equations, a mechanism diagram was made to reflect the Hg^0 removal mechanism more vividly, as shown in Figure 6. The Hg compounds were generated to be adsorbed at first after the adsorbed Hg^0 was oxidized in various ways. Then most of the oxidized mercury became gaseous finally. The adsorbed mercury that was identified was only a small amount of remaining part. Nevertheless, it was of great value for the analysis on the mechanism of the Hg^0 removal process.

4. Conclusions

The Hg-TPD analysis, together with Hg content measurement and sequential extraction procedure, was carried out to identify the mercury species and content in the spent Mn-based SCR catalysts for the purpose of acquiring related Hg^0 removal mechanism and information on the disposal of the retired catalysts. The analysis results demonstrated that the Hg^0 adsorption process was a necessity for the Hg^0 removal over the catalysts, and it was realized mainly through chemisorption, though the mercury adsorption amount accounted for only a small proportion of the Hg^0 removal efficiency and the Hg^0 oxidation was the main way for the catalysts to remove Hg^0. In simulated coal combustion flue gases, HgO was the predominant species formed in the catalysts, and a little amount of $HgCl_2$, $Hg(NO_3)_2$ and Hg-OM was also adsorbed. The components of O_2, HCl, NO and high concentration of CO_2 in the flue gases contributed to the Hg^0 removal efficiency by promoting the Hg^0 oxidation to form related Hg compounds. But similar phenomenon was not detected for SO_2, NH_3 and H_2O, and they meanwhile prejudiced the forming of HgO so that they inhibited the efficiency. As most of the adsorbed mercury was mobile, it was necessary to pretreat the spent catalysts with the solution of 2%HCl+10%ethanol to remove the mobile Hg before the disposal of them in the environment for the environmental protection.

Acknowledgments

This research was supported by the National Key Research and Development Program of China (No. 2016YFB0600604), the International Cooperation Program I-COOP+ (COOPA20174), the National Nature Science Foundation of China (NSFC) (No. 41672148) and the China Postdoctoral Science Foundation (2017M620319). The authors acknowledge the Analysis and Test Center of Huazhong University of Science & Technology.

References

(1) Díaz-Somoano, M. Minimization of Hg and trace elements during coal combustion and gasification processes. Chapter 3 in book: New trends in coal conversion, combustion, gasification, emission and coking. *Woodhead Publishing – Elsevier* **2019**, 59-88.

(2) Presto, A. A.; Granite, E. J. Survey of catalysts for oxidation of mercury in flue gas. *Environ. Sci. Technol.* **2006**, *40*, 5601-5609.

(3) Zhao, Y.; Yang, J.; Ma, S.; Zhang, S.; Liu, H.; Gong, B.; Zhang, J.; Zheng, C. Emission controls of mercury and other trace elements during coal combustion in China: a review. *Int. Geol. Rev.* **2018**, *60*, 638-670.

(4) Li, Y.; Zhang, J.; Zhao, Y.; Zheng, C. Volatility and speciation of mercury during pyrolysis and gasification of five Chinese coals. *Energy Fuels* **2011**, *25*, 3988-3996.

(5) Yang, J.; Ma, S.; Zhao, Y.; Li, H.; Zhang, J.; Zheng, C. Elemental mercury removal from flue gas over TiO_2 catalyst in an internal-illuminated honeycomb photoreactor. *Ind. Eng. Chem. Res.* **2018**, *57*, 17348−17355.

(6) Galbreath, K. C.; Zygarlicke, C. J. Mercury speciation in coal combustion and gasification flue gases. *Environ. Sci. Technol.* **1996**, *30*, 2421-2426.

(7) Zhang, B.; Xu, P.; Qiu, Y.; Yu, Q.; Ma, J.; Wu, H.; Luo, G.; Xu, M.; Yao, H. Increasing oxygen functional groups of activated carbon with non-thermal plasma to enhance mercury removal efficiency for flue gases. *Chem. Eng. J.* **2015**, *263*, 1-8.

(8) Pudasainee, D.; Kim, J.-H.; Yoon, Y.-S.; Seo, Y.-C. Oxidation, reemission and mass distribution of mercury in bituminous coal-fired power plants with SCR, CS-ESP and wet FGD. *Fuel* **2012**, *93*, 312-318.

(9) Ma, J.; Li, C.; Zhao, L.; Zhang, J.; Song, J.; Zeng, G.; Zeng, G.; Zhang, X.; Xie, Y. Study on removal of elemental mercury from simulated flue gas over activated coke treated by acid. *Appl. Surf. Sci.* **2015**, *329*, 292-300.

(10) Bae, K.-M.; Kim, B.-J.; Park, S.-J. Overlook of carbonaceous adsorbents and processing methods for elemental mercury removal. *Carbon lett.* **2014**, *15*, 238-246.

(11) Yang, J.; Zhu, W.; Qu, W.; Yang, Z.; Wang, J.; Zhang, M.; Li, H. Selenium functionalized metal-organic framework MIL-101 for efficient and permanent sequestration of mercury. *Environ. Sci. Technol.* **2019**, https://doi.org/10.1021/acs.est.8b06321.

(12) Granite, E. J.; Pennline, H. W.; Hargis, R. A. Novel sorbents for mercury removal from flue gas. *Ind. Eng. Chem. Res.* **2000**, *39*, 1020-1029.

(13) Gao, W.; Liu, Q.; Wu, C.-Y.; Li, H.; Li, Y.; Yang, J.; Wu, G. Kinetics of mercury oxidation in the presence of hydrochloric acid and oxygen over a commercial SCR catalyst. *Chem. Eng. J.* **2013**, *220*, 53-60.

(14) Li, H.; Li, Y.; Wu, C.-Y.; Zhang, J. Oxidation and capture of elemental mercury over SiO_2-TiO_2-V_2O_5 catalysts in simulated low-rank coal combustion flue gas. *Chem. Eng. J.* **2011**, *169*, 186-193.

(15) Li, H.; Wu, C.-Y,; Li, Y.; Zhang, J. CeO_2-TiO_2 catalysts for catalytic oxidation of elemental mercury in low-rank coal combustion flue gas. *Environ. Sci. Technol.* **2011**, *45*, 7394-7400.

(16) Li, H.; Wu, C.-Y.; Li, Y.; Zhang, J. Superior activity of MnO_x-CeO_2/TiO_2 catalyst for catalytic oxidation of elemental mercury at low flue gas temperatures. *Appl. Catal., B* **2012**, *111-112*, 381-388.

(17) Xu, W.; Wang, H.; Zhou, X.; Zhu, T. CuO/TiO_2 catalysts for gas-phase Hg^0 catalytic oxidation. *Chem. Eng. J.* **2014**, *243*, 380-385.

(18) Kim, M. H.; Ham, S.-W.; Lee, J.-B. Oxidation of gaseous elemental mercury by hydrochloric acid over $CuCl_2$/TiO_2-based catalysts in SCR process. *Appl. Catal., B* **2010**, *99*, 272-278.

(19) Zhang, S.; Zhao, Y.; Wang, Z.; Zhang, J.; Wang, L.; Zheng C. Integrated removal of NO and mercury from coal combustion flue gas using manganese oxides supported on TiO_2. *J. Environ. Sci.* **2017**, *53*, 141-150.

(20) Zhang, S.; Zhao, Y.; Yang, J.; Zhang, Y.; Sun, P.; Yu, X.; Zhang, J.; Zheng, C. Simultaneous NO and mercury removal over MnO_x/TiO_2 catalyst in different atmospheres. *Fuel Process. Technol.* **2017**, *166*, 282-290.

(21) Zhang, S.; Zhao, Y.; Yang, J.; Zhang, J.; Zheng, C. Fe-modified MnO_x/TiO_2 as the SCR catalyst for simultaneous removal of NO and mercury from coal combustion flue gas. *Chem. Eng. J.* **2018**, *348*, 618-629.

(22) Zhang, S.; Zhao, Y.; Díaz-Somoano, M.; Yang, J.; Zhang, J. Synergistic mercury removal over the $CeMnO_3$ perovskite structure oxide as a selective catalytic reduction catalyst from coal combustion flue gas. *Energy Fuels* **2018**, *32*, 11785-11795.

(23) Scala, F.; Anacleria, C.; Cimino, S. Characterization of a regenerable sorbent for high temperature elemental mercury capture from flue gas. *Fuel* **2013**, *108*, 13-18.
(24) Scala, F.; Cimino, S. Elemental mercury capture and oxidation by a regenerable manganese-based sorbent: The effect of gas composition. *Chem. Eng. J.* **2015**, *278*, 134-139.
(25) Rumayor, M.; Díaz-Somoano, M.; López-Antón, M. A.; Martínez-Tarazona, M. R. Mercury compounds characterization by thermal desorption. *Talanta* **2013**, *114*, 318-322.
(26) Rumayor, M.; López-Antón, M. A.; Díaz-Somoano, M.; Maroto-Valer, M. M.; Richard, J.-H.; Biester, H.; Martínez-Tarazona, M. R. A comparison of devices using thermal desorption for mercury speciation in solids. *Talanta* **2016**, *150*, 272-277.
(27) Rumayor, M.; López-Antón, M. A.; Díaz-Somoano, M.; Martínez-Tarazona, M. R. A new approach to mercury speciation in solids using a thermal desorption technique. *Fuel* **2015**, *160*, 525-530.
(28) Luo, G.; Yao, H.; Xu, M.; Gupta, R.; Xu, Z. Identifying modes of occurrence of mercury in coal by temperature programmed pyrolysis. *Proc. Combust. Inst.* **2011**, *33*, 2763–2769.
(29) Rumayor, M.; Díaz-Somoano, M.; López-Antón, M. A.; Martínez-Tarazona, M. R. Application of thermal desorption for the identification of mercury species in solids derived from coal utilization. *Chemosphere* **2015**, *119*, 459-465.
(30) Fernández-Miranda, N.; Rumayor, M.; López-Antón, M. A.; Díaz-Somoano, M.; Martínez-Tarazona, M. R. Mercury retention by fly ashes from oxy-fuel processes. *Energy Fuels* **2015**, *29*, 2227-2233.
(31) Rumayor, M.; Díaz-Somoano, M.; López-Antón, M. A.; Ochoa-González, R.; Martínez-Tarazona, M. R. Temperature programmed desorption as a tool for the identification of mercury fate in wet-desulphurization systems. *Fuel* **2015**, *148*, 98-103.
(32) López-Antón, M. A.; Rumayor, M.; Díaz-Somoano, M.; Martínez-Tarazona, M. R. Influence of a CO_2-enriched flue gas on mercury capture by activated carbons. *Chem. Eng. J.* **2015**, *262*, 1237-1243.
(33) Rallo, M.; Fuente-Cuesta, A.; López-Antón, M. A.; Díaz-Somoano, M.; Martínez-Tarazona, M. R.; Maroto-Valer, M. M. Speciation of Hg retained in gasification biomass chars by temperature-programmed decomposition. *Fuel Process. Technol.* **2014**, *126*, 1-4.
(34) Rumayor, M.; Fernández-Miranda, N.; López-Antón, M. A.; Díaz-Somoano, M.; Martínez-Tarazona, M. R. Application of mercury temperature programmed desorption (HgTPD) to ascertain mercury/char interactions. *Fuel Process. Technol.* **2015**, *132*, 9-14.
(35) Quirós-Álvarez, M.; Díaz-Somoano, M.; Bongartz, W.; Vinjarapu, S. Mercury interaction on modified activated carbons under oxyfuel combustion conditions. *Energy Fuels* **2018**, *32*, 5405-5408.
(36) Rumayor, M.; Gallego, J. R.; Rodríguez-Valdés, E.; Díaz-Somoano, M. An assessment of the environmental fate of mercury species in highly polluted brownfields by means of thermal desorption. *J. Hazard. Mater.* **2017**, 325, 1-7.

(37) Zhou, Z.; Liu, X.; Zhao, B.; Shao, H.; Xu, Y.; Xu, M. Elemental mercury oxidation over manganese-based perovskite-type catalyst at low temperature. *Chem. Eng. J.* **2016**, *288*, 701-710.

(38) Wang, F.; Li, G.; Shen, B.; Wang, Y.; He, C. Mercury removal over the vanadia-titania catalyst in CO_2-enriched conditions. *Chem. Eng. J.* **2015**, *263*, 356-363.

(39) Yang, J.; Zhao, Y.; Chang, L.; Zhang, J.; Zheng, C. Mercury adsorption and oxidation over cobalt oxide loaded magnetospheres catalyst from fly ash in oxyfuel combustion flue gas. *Environ. Sci. Technol.* **2015**, *49*, 8210-8218.

(40) Fernández-Miranda, N.; López-Antón, M. A.; Díaz-Somoano, M.; Martínez-Tarazona, M. R. Effect of oxy-combustion flue gas on mercury oxidation. *Environ. Sci. Technol.* **2014**, *48*, 7164-7170.

(41) Morris, E. A.; Kirk, D. W.; Jia, C. Q.; Morita, K. Roles of sulphuric acid in elemental mercury removal by activated carbon and sulphur-impregnated activated carbon. *Environ. Sci. Technol.* **2012**, *46*, 7905-7912.

(42) Yang, J.; Zhao, Y.; Liang, S.; Zhang, S.; Ma, S.; Li, H.; Zhang, J.; Zheng, C. Magnetic iron-manganese binary oxide supported on carbon nanofiber ($Fe_{3-x}Mn_xO_4$/CNF) for efficient removal of Hg^0 from coal combustion flue gas. *Chem. Eng. J.* **2018**, *334*, 216-224.

(43) Yang, Y.; Liu, J.; Zhang, B.; Liu, F. Density functional theory study on the heterogeneous reaction between Hg^0 and HCl over spinel-type $MnFe_2O_4$. *Chem. Eng. J.* **2017**, *308*, 897-903.

(44) Wang, Y.; Shen, B.; He, C.; Yue, S.; Wang, F. Simultaneous removal of NO and Hg^0 from flue gas over Mn-Ce/Ti-PILCs. *Environ. Sci. Technol.* **2015**, *49*, 9355-9363.

(45) Kamata, H.; Ueno, S.; Naito, T.; Yukimura, A. Mercury oxidation over the $V_2O_5(WO_3)/TiO_2$ commercial SCR catalyst. *Ind. Eng. Chem. Res.* **2008**, *47*, 8136-8141.

(46) Zhang, B.; Liu, J.; Yang, Y.; Chang, M. Oxidation mechanism of elemental mercury by HCl over MnO_2 catalyst: Insights from first principles. *Chem. Eng. J.* **2015**, *280*, 354-362.

(47) Wang, Z.; Liu, J.; Yang, Y.; Liu, F.; Ding, J. Heterogeneous reaction mechanism of elemental mercury oxidation by oxygen species over MnO_2 catalyst. *Proc. Combust. Inst.* **2018**, https://doi.org/10.1016/j.proci.2018.06.132.

(48) Zhang, M.; Wang, P.; Dong, Y.; Sui, H.; Xiao, D. Study of elemental mercury oxidation over an SCR catalyst with calcium chloride addition. *Chem. Eng. J.* **2014**, *253*, 243-250.

(49) Zhao, L.; Li, C.; Zhang, J.; Zhang, X.; Zhan, F.; Ma, J.; Xie, Y.; Zeng, G. Promotional effect of CeO_2 modified support on V_2O_5-WO_3/TiO_2 catalyst for elemental mercury oxidation in simulated coal-fired flue gas. *Fuel* **2015**, *153*, 361-369.

586 **Table 1. The high peak, start and end temperatures of the decomposition peaks of the**
587 **reference mercury compounds**[34]

Reference Hg compounds	High peak T (℃)	Start T–end T of decomposition peak (℃)
Hg_2Cl_2	119 ± 9	60–250
$HgCl_2$	138 ± 4	90–350
Hg-OM	220 ± 5	150–300
HgS black	190 ± 11	150–280
HgS red	305 ± 12	210–340
HgO red	308 ± 1; 471 ± 5	200–360; 370–530
HgO yellow	284 ± 7; 469 ± 6	190–380; 320–530
Hg_2SO_4	295 ± 4; 514 ± 4	200–400; 410–600
$HgSO_4$	583 ± 8	500–600
$Hg(NO_3)_2{\cdot}H_2O$	215 ± 4; 280 ± 13; 460 ± 25	150–230; 230–375; 375–520
$Hg_2(NO_3)_2{\cdot}2H_2O$	264 ± 35; 427 ± 19	100–375; 376–500

588 **Table 2. Operationally defined mercury fractions**[29]

Hg fractions	Extraction solution	Individual Hg species	
F1 Mobile Hg	1:1 (v/v) 2% HCl + 10% ethanol	Inorganic Hg	$HgCl_2$
			$Hg(OH)_2$
			$Hg(NO_3)_2$
			$HgSO_4$
			HgO
			Hg^{2+} complexes
		Organic Hg	CH_3HgCl, CH_3CH_2HgCl
F2 Semi-mobile Hg	1:2 (v/v) HNO_3: Deionized water	Hg^0	
		Hg^0-Metal amalgam	
		Hg^{2+} complexes	
		Hg_2Cl_2 (minor)	
F3 Non-mobile Hg	1:6:7 (v/v/v) HCl: HNO_3: Deionized water	Hg_2Cl_2 (major)	
		HgS	
		HgSe	

589 **Table 3. Related test results of the Mn-based SCR catalysts employed for Hg^0 removal in**
590 **simulated coal combustion flue gases**

Catalyst	Hg^0 removal efficiency (%) (catalyst dosage: 0.5g)	Integral area of the desorption peak	Total Hg content (ppm)
MnTi-air	57.7±3.5	40485	0.915±0.009
MnTi-oxy	64.6±4.6	62939	1.177±0.012
FeMnTi-air	73.5±2.6	66274	1.354±0.017
CMO-air	80.9±3.8	69914	1.482±0.015

591 **Table 4. Related characterization results of the Mn-based SCR catalysts**[21,22]

Catalyst	BET Surface Area (m^2/g)	Pore Volume (cm^3/g)	Pore Size (nm)	O (AC%)	O_{ad}[a]/(O_{latt}[b]+O_{ad}) (%)
MnO_x/TiO_2	122.63	0.245	62.20	65.3	30.0
Fe-MnO_x/TiO_2	127.26	0.175	56.77	68.8	34.4
$CeMnO_3$	10.13	0.059	23.83	64.5	67.2

592 [a] O_{ad}, chemisorbed oxygen. [b] O_{latt}, lattice oxygen.

593 **Table 5. Related test results of the $CeMnO_3$ catalysts employed for Hg^0 removal in individual flue gas components**
594 **and simulated coal combustion flue gases**

Reaction gas for the previous Hg^0 removal experiments	Hg^0 removal efficiency (%) (catalyst dosage (g))	Integral area of the desorption peak	Total Hg content (ppm)
Pure N_2	37.6±2.4 (0.1)	19524	0.515±0.005
N_2+4%O_2	69.1±1.8 (0.1)	34965	0.945±0.009
N_2+4%O_2+10ppmHCl	92.5±2.7 (0.1)	34194	0.922±0.008
N_2+4%O_2+400ppmSO_2	58.5±2.9 (0.1)	23268	0.674±0.012
N_2+4%O_2+400ppmNO	86.2±1.6 (0.1)	37159	1.035±0.016
N_2+4%O_2+400ppmNO+400ppmNH_3	67.1±3.5 (0.1)	29366	0.829±0.008
N_2+4%O_2+10%H_2O	/	30561	0.816±0.007
N_2+4%O_2+12%CO_2	/	34095	0.934±0.005
N_2+4%O_2+70%CO_2	/	40352	1.066±0.018
N_2+4%O_2+12%CO_2+10ppmHCl+400ppmSO_2 +400ppmNO+400ppmNH_3	88.4±3.2 (0.5)	/	/
N_2+4%O_2+12%CO_2+10ppmHCl+400ppmSO_2 +400ppmNO+400ppmNH_3+10%H_2O	80.9±3.8 (0.5)	69914	1.482±0.015
N_2+4%O_2+70%CO_2+10ppmHCl+400ppmSO_2 +400ppmNO+400ppmNH_3+20%H_2O	83.2±4.3 (0.5)	/	/

595 **Table 6. Total mercury contents of the Mn-based SCR catalysts spent in simulated coal**
596 **combustion flue gases after the extraction of F1**

Catalyst	Total Hg content (ppm)	Decline of the content (%)
MnTi-air	0.088±0.006	90.4
MnTi-oxy	0.171±0.021	85.5
FeMnTi-air	0.123±0.008	90.9
CMO-air	0.113±0.003	92.4

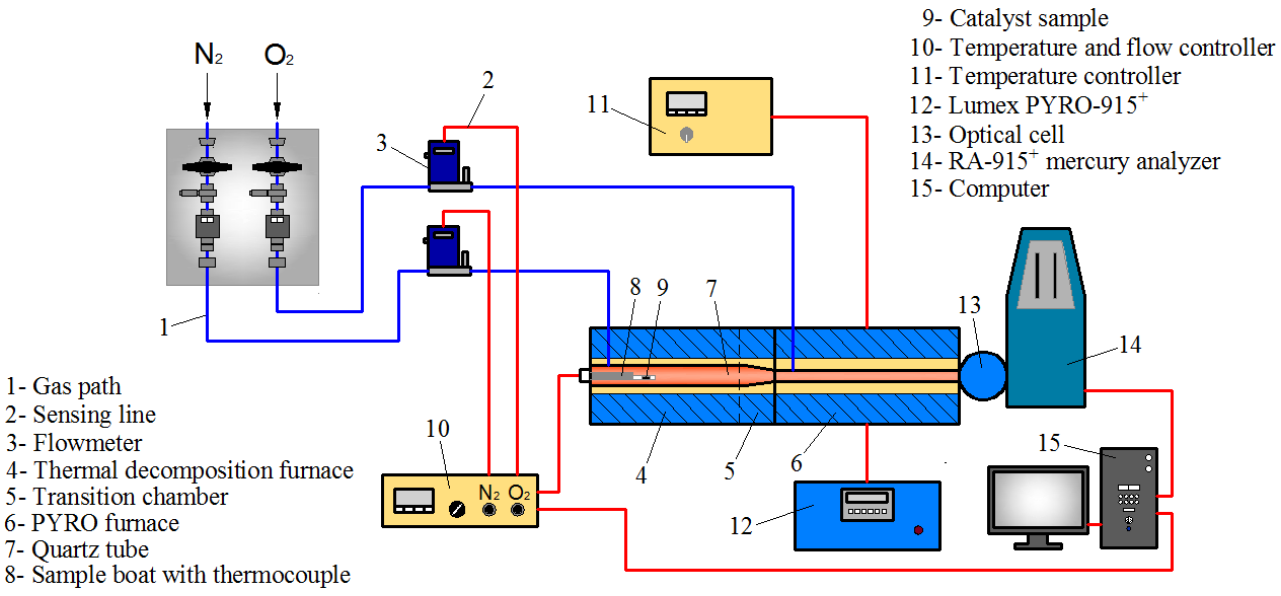

Figure 1. Schematic diagram of the Hg-TPD analytical system.

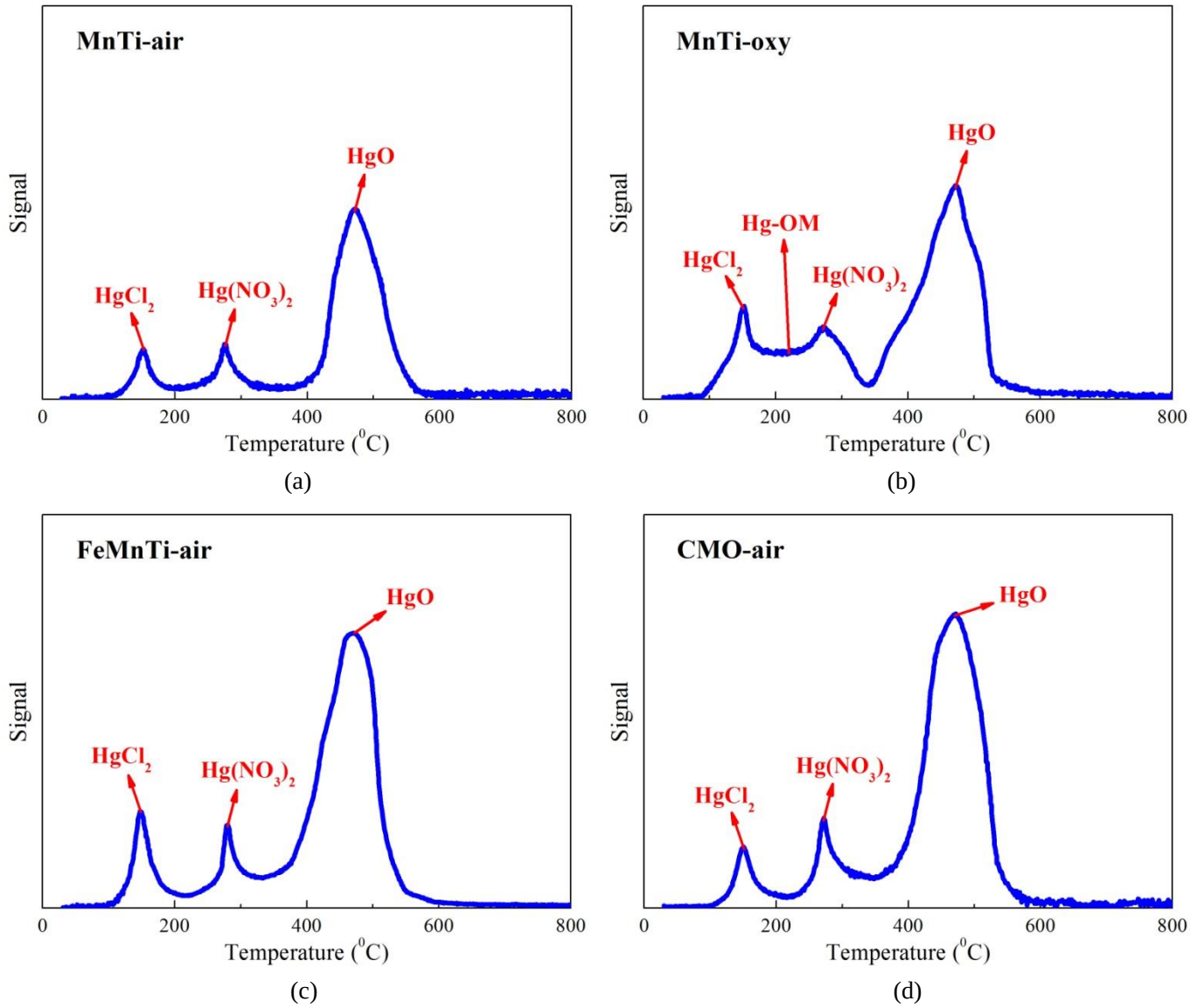

Figure 2. Mercury thermal decomposition profiles of the Mn-based SCR catalysts spent in simulated coal combustion flue gases ((a) MnTi-air, (b) MnTi-oxy, (c) FeMnTi-air and (d) CMO-air).

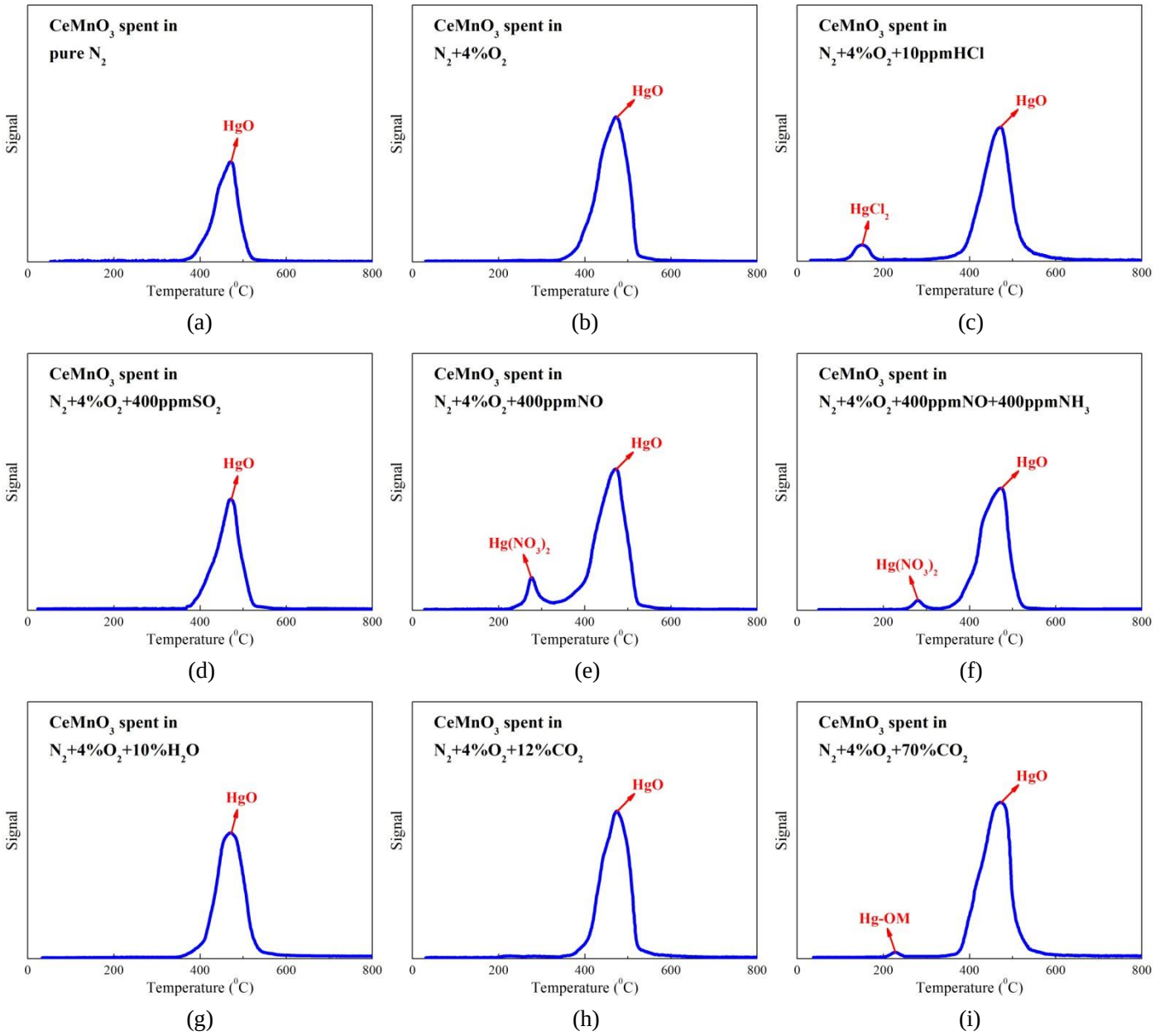

Figure 3. Mercury thermal decomposition profiles of the $CeMnO_3$ catalysts spent in individual flue gas components (spent in (a) pure N_2, (b) N_2+4%O_2, (c) N_2+4%O_2+10ppmHCl, (d) N_2+4%O_2+400ppmSO_2, (e) N_2+4%O_2+400ppmNO, (f) N_2+4%O_2+400ppmNO+400ppmNH_3, (g) N_2+4%O_2+10%H_2O, (h) N_2+4%O_2+12%CO_2 and (i) N_2+4%O_2+70%CO_2).

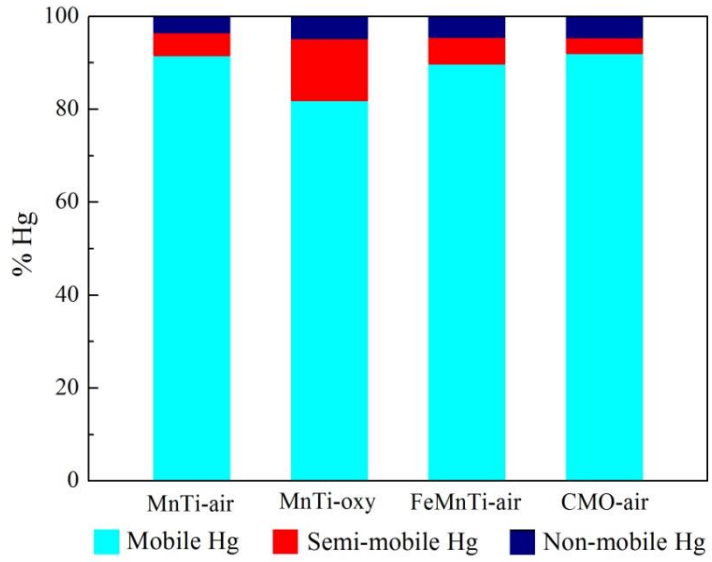

614

615 **Figure 4.** Mercury fractionation in the Mn-based SCR catalyst samples spent in simulated coal
616 combustion flue gases.

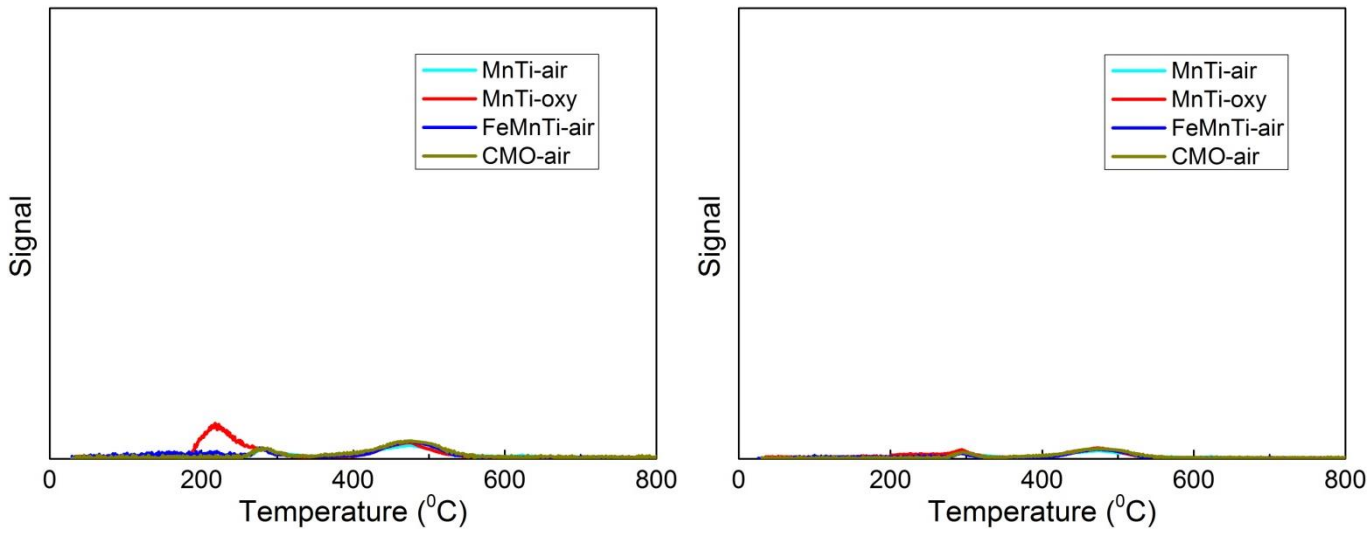

Figure 5. Mercury thermal decomposition profiles of the spent Mn-based SCR catalysts after the extraction of (a) F1 and (b) F3.

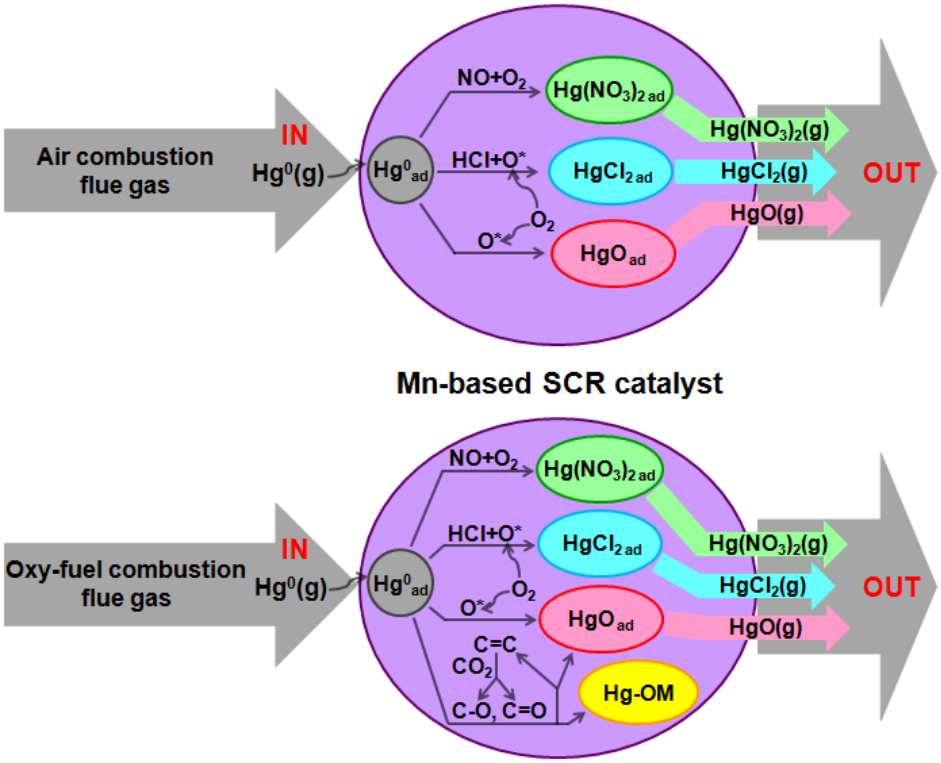

621

622 **Figure 6.** Description on the mechanism of Hg^0 removal over the Mn-based SCR catalysts in coal
623 combustion flue gas.